Construction and Building Materials 185 (2018) 325–337

Contents lists available at ScienceDirect

Construction and Building Materials

journal homepage: www.elsevier.com/locate/conbuildmat

Investigation and evaluation of railway ballast properties variation during technological processes

Deividas Navikas [a,b,*], Henrikas Sivilevičius [a], Matas Bulevičius [c]

[a] Department of Mobile Machinery and Railway Transport, Vilnius Gediminas Technical University, Plytines str. 27, LT-10105 Vilnius, Lithuania
[b] Department of Automobile Transport Engineering, Vilnius College of Technologies and Design, Antakalnio str. 54, LT-10303 Vilnius, Lithuania
[c] JSC "Granitinė skalda", Granito str. 2, LT-02241 Vilnius, Lithuania

HIGHLIGHTS

- Variation of railway ballast properties increasing during technological process.
- Aggregates segregation during technological process increase gradation variation.
- Sampling during technological process are assessed by statistical indicators.
- Principle of max standard deviation of aggregates allow compare its homogeneity.
- Compulsory sample size increase then homogeneity of railway ballast decreases.

ARTICLE INFO

Article history:
Received 17 October 2016
Received in revised form 4 July 2018
Accepted 11 July 2018
Available online 18 July 2018

Keywords:
Railway track
Ballast
Gradation
Transporter belt
Plant stockpile
Wagon
Layer
Homogeneity
Normal distribution
Sample size

ABSTRACT

Railway ballast (RB) layer has to limit tie movement by resisting vertical, lateral and longitudinal forces from the train and the track, to reduce the stresses from train loads applied to the subgrade, thus limiting permanent settlement. It also has to provide immediate water drainage from the track structure, to aid in alleviating frost problems, to facilitate maintenance surfacing and lining operations, to provide support for ties with the necessary resilience to absorb shock from dynamic loads. Secondary functions include retarding vegetation and resisting effects of fouling from surface deposited materials, absorbing airborne noise, providing adequate electrical resistance between rails, facilitating the redesign or reconstruction of the track. These properties are obtained through the use of proper gradation crushed granite, by determining its proper laying and compacting technological parameters, by ensuring sufficient thickness and profile of the layer. This paper presents statistical investigations of the four samples of crushed granite taken from transporter belt (TB), plant stockpile (PS), wagon (W) and railway construction (RC) uncompacted layer used to RB course. The gradation (particle size distribution), density of crushed granite particles (DEN_P), water absorption (WA_{24}), Deval index (M_{DE}), Los Angeles coefficient (LA_{RB} coefficient) and resistance to crushing (SZ_{RB}) of four samples were measured. Statistical parameters of crushed granite qualitative indicators, histograms, theoretical curves of normal distribution are presented. Their compliance with normal distribution was verified by employing the criteria of skewness, kurtosis, Pearson, Shapiro-Wilk and Kolmogorov-Smirnov. Dependance of standard deviations of percent passing through sieves on the means of percent passing through these sieves was obtained from regression analysis. The use of Kruskal-Wallis test by ranks showed that means obtained in different sample-taking locations did not differ statistically. The maximum value of standard deviation of this dependance, equal to mean of 50% percent passing, was used to evaluate the homogeneity of crushed granite used to construct the ballast layer according to the variation of its gradation. Absolute allowable error of minimum sample size *n*, equal to 5%, 10%, 15% and 20%, was calculated. Investigation results indicated that due to segregation the homogeneity of the gradation of crushed granite used to construct the ballast layer from its production site to its exploitation site decreased by 78%. During the technological processes of loading, transporting and spreading the gradation has hardly changed.

* Corresponding author at: Department of Mobile Machinery and Railway Transport, Vilnius Gediminas Technical University, Plytines str. 27, LT-10105 Vilnius, Lithuania.
E-mail address: deividas.navikas@vgtu.lt (D. Navikas).

https://doi.org/10.1016/j.conbuildmat.2018.07.090
0950-0618/

1. Introduction

In Lithuania railway transport is a one of the leading GDP (Gross Domestic Product) producer among all transport modes. The length of the railway in Lithuania makes up 1767.6 km [1], and it is very important to maintain the existing and newly constructed tracks in its best possible condition. Railways have many advantages over other transport modes and, as a result, the industry has experienced a significant growth in terms of both passenger numbers and freight tonnage.

The choice of a particular mode of transport as an alternative to another one is subjective and usually based on an individual passenger's approach to the evaluation of advantages and disadvantages of some particular means of transport [2]. The paper presents the methods of analysing the reasons for passengers choice travelling by train as an alternative to using air transport and the results obtained in the research. The weight of five subcriteria making the "ride comfort" criterion group was equal to 0.3865 (the largest overall weight).

Railroad construction quality is important as much as railway trains and wagons technical quality for moving loads and passengers trip quality and safety [3,4].

In railroad construction ballast and sub-ballast play a significant role. Railroad ballast has to resist vertical and longitudinal forces, to hold the track in position, to provide energy absorption for the track, to facilitate adjustment of the track geometry, to provide immediate drainage of water falling onto the track, to reduce pressures on underlying materials by distributing loads and to provide energy absorption for the track [5].

Railway track ballast, sub-ballast and railway bed, impacted by the factors of train traffic loading, climate and ambient air, deform, due to which track quality index (TQI) varies [6–8]. The life of ballast depends upon a number of factors, mainly traffic loading, drainage, contamination, and is clearly related to intervention levels and installation quality standards [9].

From the economic standpoint, the cost of fuel consumed by railway transport makes up one-seventh of that of the road transport. Additional advantages include low pollution and high safety levels. The main disadvantage of the high cost of repair and maintenance activity is an improper stress distribution within the foundations under the track. This problem can be caused by breakage and attrition in the ballast or deterioration of the subgrade [10–12]. Considering that, maintenance costs for rail track subsystem may represent about 55% of the total maintenance costs [13].

The whole maintenance demand of the track depends on its initial quality. However, due to a small contact area between the sleeper and the ballast (3 to 5%), initial settlements by cracking of the ballast are unavoidable. As long as the ballast stones cannot bear the concentrated forces, cracking will occur, until more and more stones come into contact, which increases the contact area. Unfortunately, these initial settlements are not similar but differ from sleeper to sleeper, which forms initial failures, causing dynamic forces, increasing the failures, increasing the forces, and so on and finally causing the need for maintenance. The consequences of ballast wear are therefore vertical alignment failures and pollution of ballast bed. In principle, in order to improve the situation, two solutions exist: first, to increase the quality of ballast and second, to reduce forces in ballast [14].

Ballast is mostly produced from natural deposits of granite, trap rock, quartzite, dolomite, limestone or other natural soils. Railway ballast is generally composed of uniformly graded angular aggregate. As ballast ages, it can be progressively fouled by numerous fine materials, the accumulation of which in the voids of ballast can result in a decrease in shear strength with reduced resiliency and drainage capability of the ballast [5]. Ballast materials forming part of railway structures are subjected to cyclic loads. As a result of these loads, ballast densification, aggregate degradation, and lateral spread of the ballast material underneath the ties take place inducting permanent deformations on the railways [15].

The degradation of track geometry induces an evolution of the initial gradation and angularity due to fouling or numerous maintenance operations. The usual process for track or ballast renewal is based on some investigations about the track geometry and substructure and the efficiency of maintenance operations [16]. The bearing capacity depends on the qualities and thicknesses of soils that compose the subgrade, from the formation layer to the lower layers. These models can establish the tensional and deformation state of each cross-section of materials and layer, which is an important tool in the design phase of railway track [17]. The migration of particles and the interaction between ballast and sub-soil layers are one of the biggest problems in exploiting roads [18]. Substructure instability can be caused by weak subgrade soils, ballast breakdown, poor-quality ballast, thickness of the ballast and top formation layers. Sources of ballast fouling consist of ballast particle degradation, infiltration of fine foreign particles from the track surface, sleeper wear, as well as sub-ballast and subgrade infiltration [19].

The instability of railway components may be caused by too weak building materials used, ballast fragmentation, its poor quality, insufficient thickness of ballast and other materials used in the layers. Ballast decline is caused by ballast particle degradation, penetration of other materials into the layer, wear of rails as well as mixing of ballast and sub-ballast layer materials [19].

The obtained results [20] confirmed that for impact-load components over 100 Hz, the ballast layer resists because of its high rigidity and can reduce the impact loads substantially. However, the ballast layer is almost non-resistant to the low-frequency load components, which are not reduced enough.

Kennedy et al. [21] presents the measured settlement results of full-scale testing of unreinforced and polymer-reinforced ballast railway track under laboratory conditions. The measured settlement profile of each track specimen is monitored up to a maximum of 500.000 load cycles at different load levels and formation conditions. The polymer treated track is observed to reduce permanent track settlement by 99%, effectively giving slab-track like performance.

The obtained results [22] indicate that the use of 10% of crumb rubber (by volume) could reduce ballast degradation and at the same time as the capacity of the ballast layer to dissipate energy is increased, its stiffness is reduced as well. Additionally, based on the present laboratory study, the track settlement could be reduced with 10% rubber particles used as elastic aggregates.

Execution of tamping is highly dependent on the condition data and there is no well-structured track degradation analysis that helps to make long-term maintenance plans. The evaluation of the standard deviation for the longitudinal level at which tamping is executed indicates that the execution of tamping is not optimally planned ([23,24].

Caetano and Teixeira [25] propose a railway track geometry degradation model that considers uncertainties in the forecast by defining a track geometry reliability parameter. The degradation model integrated in a multiobjective optimization approach assesses railway track maintenance strategies considering cost-reliability trade-off.

The Bayesian model for rail track geometry degradation allows to asses the evolution of uncertainty associated with degradation parameters throughout the rail track life-cycle. Prior probability distributions were fitted to track geometry degradation, showing that Log-Normal distribution is the most suitable distribution to model deterioration parameters [26].

Railway road geometry degradation (the Bayesian model) enables to evaluate uncertainty related to degradation parameters throughout the whole railway life-cycle. Advanced probability distributors were applied to evaluate road geometry degradation, which show that the best applicable distribution model to evaluate degradation parameters is Log-Normal distribution [26].

The test of correlation between quality indices of different aggregate strains and its strength indices determined a strong correlation between all values of FI (flakiness) and SI (shape indexes), as well as dolomite aggregate indices FI and LA (Los Angeles coefficient). The analysis of correlation dependence between geometrical and strength indices of different rock samples showed a significant decline of particle strength, when the number of flat and oblong particles was greater ([27–29].

Aggregate resistance to polishing and degradation can be related to the change in some of those aggregates particle characteristics. Polishing resistance can be related to the loss of surface texture [30].

Yideti et al. [31] presented the packing theory-based framework for unbound granular materials composed of stones with a size distribution described through a gradation analysis.

For the hydraulic behaviour, a large-scale cell was developed allowing drainage and evaporation tests to be carried out with monitoring of both suction and volumetric water content at various positions of the sample. The hydro-mechanical behaviour of fouled ballast was carried out by infiltration tests and triaxial tests under both monotonic and cyclic loadings. Water content and fines content effect on the hydraulic behaviour. The effect of water content on the hydraulic behaviour was found similar to that for common unsaturated soils. The hydraulic conductivity decreases with increasing suction [32].

The experimental, numerical, and field investigations confirm that high frequency shocks causing accelerated breakage of ballast shock mats in track could offer an attractive solution for enhanced performance of ballast through impact attenuation and subsequent mitigation of ballast degradation. A shock mat placed at the bottom of the ballast offers enhanced performance through reduced breakage and track settlement; whereas for relatively softer subgrades, the shock mat offers optimum protection if it is ideally placed at the top of the ballast [33].

The ballast with relatively low confining pressure often exhibits high stress dilatancy and particle breakage behaviour during loading. Particle breakage within the tested sample inevitably changes the particle gradation of the ballast. To predict the stress–strain response as well as the gradation evolution of the ballast under relatively low confining pressure, a specific bounding surface model is proposed by employing a modified particle breakage variable, which correlates the initial gradation and the ultimate gradation together with the current gradation [34]. Ballast breakage is identified as the most significant source of fouling, while it is known that the degradation of particles influences the strength and deformation behaviour of granular media [35]. The intrusion of coal fines into the ballast layer significantly reduces its shear strength, and may cause rapid track deterioration along with a need for more regular maintenance. The results of triaxial tests indicated that the shear strength of ballast was greatly reduced due to the addition of an appreciable amount of coal fines [36].

If particle shape, particle-size and relative density are considered in a proper manner, a relatively simple constitutive law with only three constants (friction coeficient, shear and normal stiffness) is sufficient for the reproduction of the observed stress-deformation behaviour [37]. The critical-state friction angle decreased with an increase of the consolidated pressure. The particle breakage during specimen compaction had more significant influence on the position of the breakage critical-state line (BCSL) in the line up plane than the particle breakage during shearing [38].

The work aims to estimate the statistical parameters of physical and mechanical properties, to test and evaluate the homogeneity of the crushed railway ballast (RB) and its variation from its production site to its exploitation site by employing statistical methods. It also aims to estimate the minimum representative sample size, when samples are taken from transporter belt (TB), plant stockpile (PS), transporting wagon (W) and from uncompacted layer of railway construction (RC).

2. Investigation of ballast properties

Lithuania is a country on the territory of which there are no easily accessible granite rocks on the surface of ground (except separate stones). Therefore, crushed granite to be used for railway ballast is produced in Lithuanian plants from bulk pieces brought from other countries by railway, crushed in Lithuanian stonebreakers and sieved through technological screens of appropriate mesh.

2.1. Ballast aggregate sampling

The characteristics of aggregates used in Lithuania for ballast layer (Fig. 1.) are regulated by LST EN 13450:2013. This standard stipulates the requirements for the gradation, category and standardized properties of the material: Los Angeles (LA_{RB}) coefficient, Deval test (M_{DE}, resistance to crushing (SZ_{RB}), particle density (DEN_P), water absorption (WA_{24}), fine particle class (f_{RB} or G_F RB), by their percentage content.

A number of methods were employed to determine RB physical and mechanical properties by investigating representative sets. To identify their gradation, the produced samples of RB were taken from TB and PS. Other samples of RB transported to the site were taken from W and spread on RC. As the deposits of raw material are located rather far away from construction sites not only in Lithuania, but in other European Union (EU) countries as well, intermediate control parameters for gradation are applied by taking samples from V or RC (Table 1). Table 1 does not give standard values; therefore, the ones presented in it shall be used as reference specifications.

Inevitable crushed granite segregation processes, crumbling of its particles during its transportation and reloading are limited by maximum percent passing through 22.4 mm sieve according to the category of crushed stone (Table 1).

Standard methods were employed to determine all values of the investigated properties (Table 2).

In some countries, like Sweden and Finland, when building and exploiting railways, correction coefficients complying to the above-mentioned standards are applied, which take crumbling and segregation of crushed stone into account [40].

The research findings indicate that the properties of crushed RB from its production site to its exploitation site vary. However, its

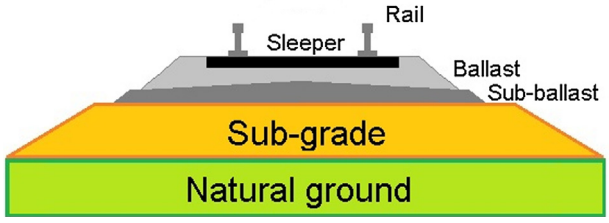

Fig. 1. Railway track structure.

Table 1
Degradation of railway ballast during transportation [39].

Test clause	Description	Category		
		A	B	C
6.2	Maximum percentage by mass passing 22.4 mm sieve	5	7	No requirement
6.2	Maximum percentage by mass passing 25 mm sieve	6	8	No requirement

Table 2
The number of RB samples taken from different locations of the technological process.

Sampling location		Index					
		Gradation	M_{DE}	DEN_P, Mg/m^3	WA_{24}, cm	SZ_{RB}	LA_{RB}
Sample size	TB	6	4	3	3	4	3
	PS	9	1	1	1	1	1
	V	32	29	26	26	29	29
	RC	16	2	2	2	2	2
	Total	63	36	32	32	36	36

Note: TB – transporter belt; PS – plant stock pile; W – wagon; RC – railway construction.

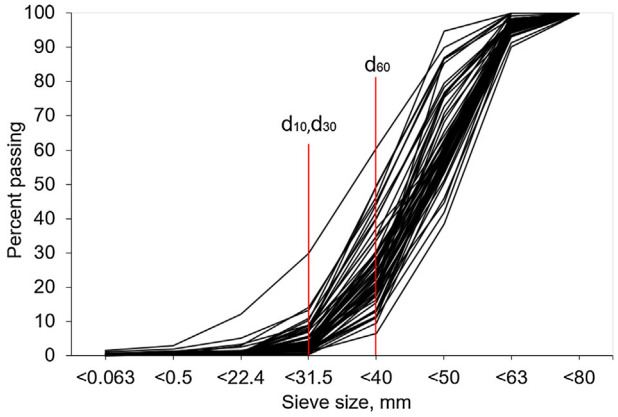

Fig. 2. Gradation of railway ballast samples taken from different technological process locations.

variation degree has been scarcely investigated and is influenced by concrete local conditions.

2.2. Gradation

Having tested 63 RB samples taken from different technological process locations, such as TB, PS, W and RC, the following gradation curves were obtained (see Fig. 2).

The estimated distribution parameters indicate that the highest standard deviation of percent passing are those of particle size of 40 and 50 mm, and the coefficient of variation is the highest of particles smaller than 31.5 mm (Table 3).

A rather wide range of distribution parameters (Std. Dev. and CoV.) indicates that RB samples taken from different stages of the technological process vary.

2.3. Uniformity coefficient of gradation curve and the rate of curvature

The properties of crushed granite may be additionally evaluated according to the requirements applied to the soil. During its exploitation, the subgrade of crushed granite mixes with the upper part of the sub-ballast layer. Therefore, the properties of these two layers' mixed area are impacted by the structure and homogeneity of crushed granite and soil mixture. It is rather difficult to evaluate these properties as their investigation has not been specified in any normative documentation.

Uniformity coefficient C_u of crushed granite is characterized by the steepness of the gradation curve within the interval from d_{10} to d_{60}. The lower the uniformity coefficient C_u of crushed granite is, the better parameters of uniformity and gradation are obtained.

The uniformity coefficient of railway crushed ballast is calculated by the following formula [41]:

$$C_u = \frac{d_{60}}{d_{10}}, \quad (1)$$

where d_{10}, d_{60} – diameter of particles, which in the ordinate of gradation curvature complies up to 10% and up to 60% of summative parts of railway ballast mass under investigation, mm. Where d_{10}, d_{60} – the particle diameter at 10% and 60% passing (respectively), mm.

The diameters of the investigated crushed RB are d_{10} = 31.5 mm and d_{60} = 40 mm; therefore, its uniformity coefficient C_u = 1.27.

The rate of curvature C_c describes the type of railway ballast gradation curvature within the interval of d_{10} and d_{60} and is calculated according to the following formula [41]:

$$C_c = \frac{(d_{30})^2}{d_{10} \cdot d_{60}}, \quad (2)$$

where d_{10}, d_{30}, d_{60} – diameter of particles, which in the gradation curvature ordinate complies with up to 10%, 30% and 60% of the railway ballast mass part under investigation, mm. Where d_{10}, d_{30}, d_{60}

Table 3
Railway ballast gradation distribution.

Statist. ind., %	Percent passing through sieves (mm)						
	0.063	0.5	22.4	31.5	40	50	63
Mean	0.28	0.49	1.02	4.83	25.52	63.62	96.5
Std. Dev.	0.26	0.5	1.64	4.41	10.98	12.3	2.16
CoV.	92.9	102	160.8	91.3	43	19.3	2.2

– the particle diameter at 10%, 30% and 60% passing (respectively), mm.

Having calculated means (Table 3) from RB gradation curves (Fig. 2), the diameters of particles, at 10%, 30% 60% passing (respectively) are $d_{10} = 31.5$ mm, $d_{30} = 31.5$ mm and $d_{60} = 40$ mm, $C_c = 0.79$. Critical values of the uniformity coefficient and the rate of curvature according to which crushed granite is classified are presented in Table 4.

The calculation results indicate that according to its uniformity coefficient value ($C_u = 1.27 < 6$), RB crushed granite is of bad curvature (B), and according to its rate of curvature ($C_c = 0.79 < 1$) it is of various (P) curvature (Table 4).

2.4. Ballast aggregate gradation classes

Large contents of fine particles (0.5 mm) and mineral dust (0.063 mm) are negative factors on RB. During the exploitation of RB, they migrate to sub-ballast layer and thereby increase the mixing of RB with sub-ballast layers. Therefore, a smaller content of these particles shall be used during the stages of RB production and exploitation. The content of fine particles (0.5 mm) and mineral dust (0.063 mm) shall be checked on the production site. Moreover, it is also recommended to verify its content during other stages of the technological process [39]. Classification of the investigated RB crushed granite samples s presented in Fig. 3.

The content of mineral dust in the investigated RB accounts for 92% of class A (Fig. 3a), and the content of fine particles accounts for 81% of class A (Fig. 3b). The data of percent passing through laboratory sieves indicate that crushed RB material of class D makes up the bulk part (57%) (Fig. 3c).

2.5. Ballast aggregate gradation variation indicator

During segregation processes the heterogeneity of crushed granite increases. Gradation variation is expressed by standard deviations s_p of percent passing through all screens. Their values depend on means $\bar{p}$of percent passing and the homogeneity of the material. It is recommended to evaluate the variation of crushed granite [42] according to value s_{pmax} of the maximum percent passing through sieves. Correlation $s_p = f(\bar{p})$, obtained from the experimental investigation of the gradation enables to calculate s_{pmax} of RB aggregate, not taking into consideration the mesh size of the laboratory sieves used. Standard deviation of percent passing varies depending on the means according to the following regression model [42]:

$$s_p = \sqrt{a \cdot \bar{p}^b \cdot \left(100 - \bar{p}\right)^c}, \quad (3)$$

where a, b, c – unknown parameters of the model (regression coefficient), influencing on the shape and asymmetry of the curve; s_p – standard deviation of percent passing through any sieve, %; $\bar{p}$– mean percent passing through this sieve, %.

The model (3) indicates that maximum s_{pmax} occurs in the particles the content of which in crushed RB material accounts for 50% of its mass.

Table 4
Classification of soils by uniformity coefficient and rate of curvature [41]

Title	Symbol	Uniformity coefficient C_u	Rate of curvature C_c
Bad curvature soil	B	<6	Any
Good curvature soil	G	≥6	$1 < C_c < 3$
Various curvature soil	P	≤6	<1 or >3

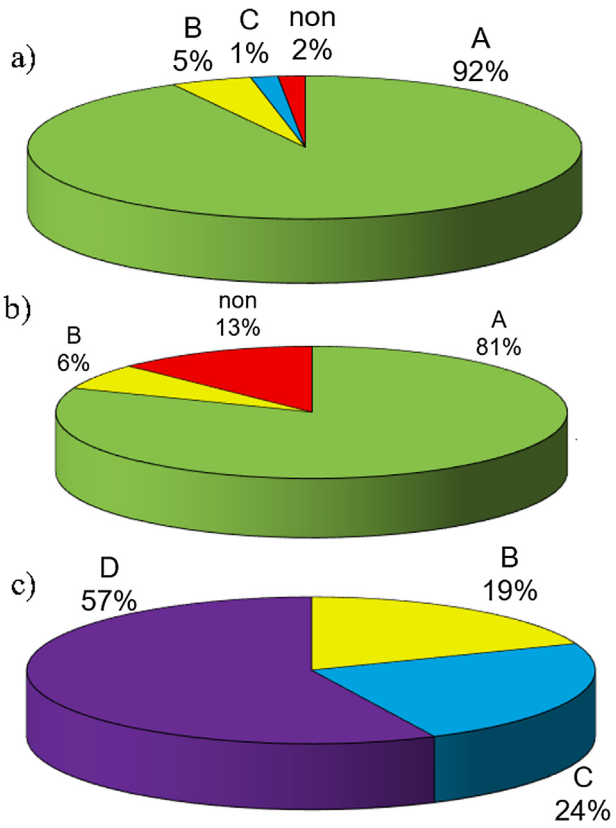

Fig.3. Results of RB sample classification: *a* – fines (0.063 mm) content category; *b* – fine particle (0.5 mm) category; *c* – RB grading category.

The following homogeneity regression equation was obtained through the use of the statistical data from 63 samples of experimental grading RB (Fig. 4).

The values of determination coefficient close to 1 ($R^2 = 0.904$) indicate that the variance of standard deviation s_p of all RB percent passing through sieves is by more than 90% influenced by the variation of mean $\bar{p}$.It follows that the obtained regression equation (Fig. 4.) is reliable, and its calculated ordinates indicate strong correlation between the characteristics of each RB gradation and may be used to evaluate the homogeneity of the gradation of the samples taken in different locations.

Statistical indicators of percent passing of the crushed RB through separate laboratory sieves, histograms and theoretical curves of normal (Gaussian) distribution are presented in Fig. 5.

The distribution of particles passing through the sieves of 40 mm, 50 mm and 63 mm mesh size is approximate to normal. The

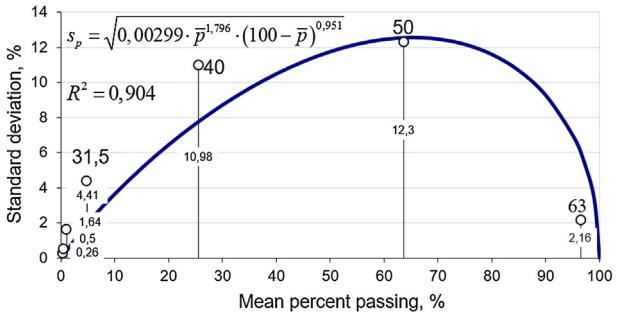

Fig. 4. Correlation between the parameters of ballast material gradation variation (s_p) and position ($\bar{p}$).

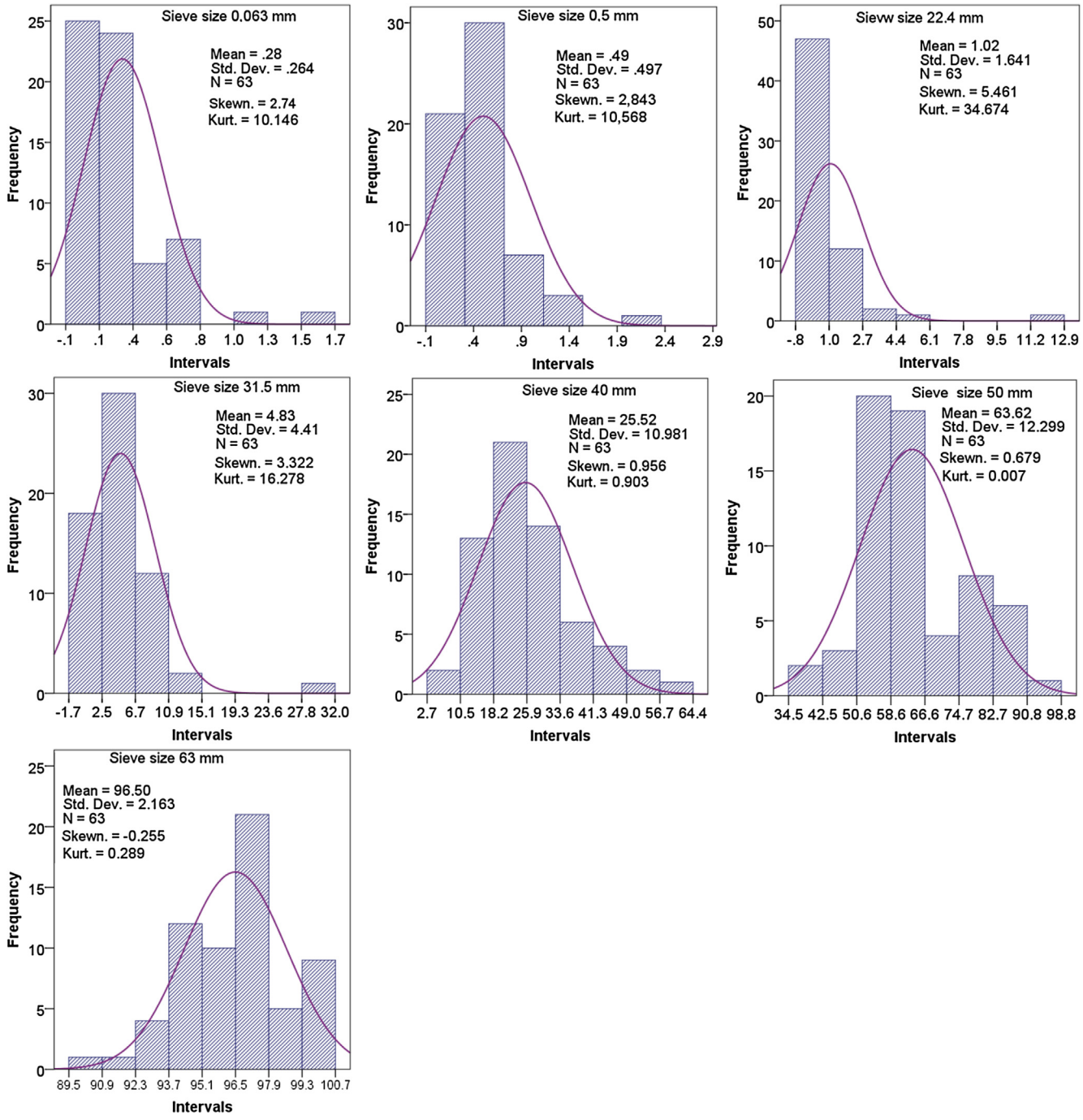

Fig. 5. Statistical indicators and histograms of ballast particles percent passing through sieves.

size of particles ranging from 0.063 mm to 31.5 mm have positive (right-hand) asymmetry as their contents in histograms are distributed on the left side of the mean: most values are on the left side of the mean (Fig. 5.).

The higher the asymmetry of experimental data, the larger departure from normal distribution is. Bartlett's criterion can be used to calculate the mean of dispersion providing the data are distributed according to normal (Gaussian) law. This criterion is very sensitive to a wide range of non-normality.

2.6. Other ballast aggregate properties

Table 1 gives the number of samples taken to investigate RB properties (M_{DE}, SZ_{RB}, LA_{RB}, DEN_P and WA_{24}). The obtained statistical parameters (Table 5) indicate that the greatest variation occurs with M_{DE} and WA_{24}, where variation coefficients are equal to 31.4% and 96.0%, respectively. It could be influenced by the heterogeneity of the rock stock, errors of sample taking and testing.

Table 5
Distribution of other railway ballast properties.

Statist. ind.	Properties				
	M_{DE}	SZ_{RB}	LA_{RB}	DEN_P	WA_{24}
Mean	5.5	16.3	12.4	2.7	0.2
Std. Dev.	1.7	1.7	2.6	0.1	0.1
CoV.	31.4	10.3	21.1	2.2	96.0

The distribution of SZ_{RB} also LA_{RB} values is symmetrical and close to normal distribution (Fig. 6). Other values of properties (M_{DE}, DEN_P and WA_{24}) have a positive (right-hand) asymmetry, as their contents in histograms are distributed on the left-hand side of the mean: most of the values are on the left-hand side of the mean (Fig. 6.).

The RB meets class 18 of resistance to crumbling (SZ_{RB}), and classes 12 and 14 of Los Angeles coefficient (LA_{RB}) (Fig. 7).

The RB resistance to crumbling was tested by employing the following two different methods: Los Angeles (LA_{RB}) method in drum and the impact method. The obtained results indicate that samples tested by two methods differ (Table 5). The results obtained from SZ_{RB} method show that crushed RB material is of higher category than it was determined through the use of LA_{RB} method (Fig. 7.).

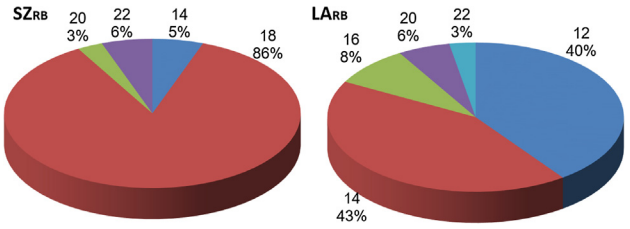

Fig. 7. Results of grouping railway ballast into classes and categories in percentage.

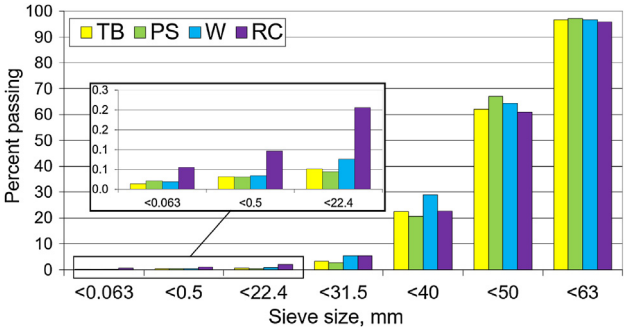

Fig. 8. Differences of means of gradation (percent passing) of RB samples taken in various locations of the technological process.

3. Railway ballast statistical indicators

3.1. Investigation of the homogeneity of sample means

Having grouped the samples by their sampling location into TB, PS, W and RC, their means were obtained (Fig. 8). As the values of means differ, it was decided to compare four means of gradation and other properties according to their sampling location by employing Kruskal Wallis test by ranks. This method is suitable to verify the homogeneity of means when the number of samples varies.

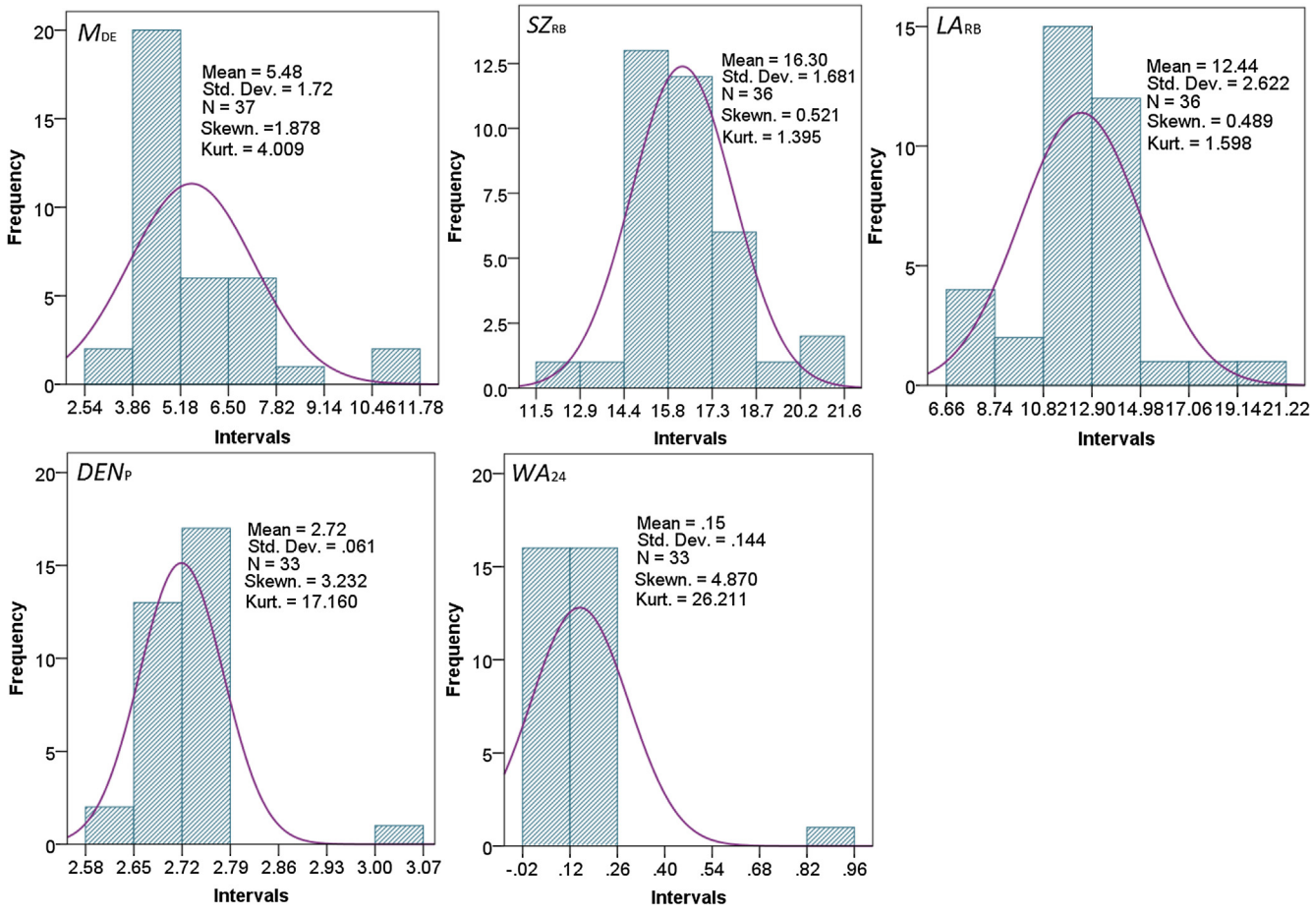

Fig. 6. Properties of RB and statistical indicators.

The rating criterion of Kruskal Wallis test by ranks is used to verify the distribution of four different sampling locations by calculating statistics [43]:

$$H = \frac{12}{n(n+1)} \cdot \sum_{j=1}^{k} \frac{r_j^2}{n_j} - 3(n+1); \quad (4)$$

where k – the number of variables; n_j – the number of observations of j variable $n = (n_1 + n_2 + \ldots + n_k)$; r_j^2 – j sample range sum squared.

When identifying the homogeneity of means of percent passing through separate laboratory sieves, the following four different sampling locations were tested: TB, PS, W and RC ($k = 4$). Sample numbers in each location are equal to $n = 6$ (TB), $n = 9$ (PS), $n = 32$ (W) and $n = 16$ (RC), respectively. (Table 2). Means of each sampling location percent passing through laboratory sieves were rated from 1 to the last number (the size of a sample) in the increasing order and sample rating sum squared (r_j^2) was calculated. The estimated statistics of β and H are presented in Table 6.

The comparison of the statistics of β values with the accepted significance level ($\alpha = 0.05$) indicates that the distribution of percent passing of particles sized from 0.063 mm to 40 mm varies ($\beta < \alpha$). Means of percent passing of 50 mm and 63 mm in four sampling locations do not vary ($\beta \geq \alpha$), as $\beta = 0.461$ and $\beta = 0.575$ are higher than $\alpha = 0.05$.

If means are the same, crushed stone by its gradation is the same from its production site to its exploitation site. The size of its separate fraction particles does not vary statistically. If means do not vary, the coarse part of the crushed granite fined down inconsiderably during the stages of the technological process.

The means of other physical and mechanical parameters of the crushed RB from four samples do not differ ($0.152 < \beta < 0.953$), as β is larger than $\alpha = 0.05$. Statistical homogeneity of the investigated physical and mechanical properties means shows that the properties of the material did not vary during the stages of the technological process.

According to Kruskal-Wallis test by ranks, the means of percent passing through laboratory sieves and other properties are the same, as H statistics of all four sample-taking locations is $\chi^2_{0.05} > H$(Table 6).

3.2. Normal distribution of results

To construct RB layer, crushed granite is used. Due to the parameters of its production technological process, in-plant stratification in a stock-pile and mixing during transportation, a certain degree of heterogeneity occurs. Its heterogeneity is shown by the parameters of gradation and other properties' dispersion (standard deviation, dispersion, variation coefficient). To compare stochastically dispersed samplings according to dispersion parameters, their compliance with the normal (Gaussian) law shall be determined.

To verify the normality of randomly taken samples, the criteria of skewness (Skew) and kurtosis (Kurt) as well as Kolmogorov-Smirnov (KS) [44], Shapiro-Wilk (SW) [45–48], Pearson (χ^2) are employed.

Table 7 gives compliances of experimental data to normal distribution obtained according to different criteria. Appendix 1 presents compliance of separate sampling locations (TB, PS, W and RC) to normal distribution.

The results of verifying the empirical (experimental) data distribution compliance to normal distribution (given in Table 7 and Appendix 1) indicate that according to Pearson (χ^2) most of the properties of all RB samples taken from separate sampling locations comply to the Gaussian distribution (Table 7, marked by "+").

Table 6
Kruskal-Wallis test rating criterion for independent samples.

Statistical indicator		Gradation (percent passing through sieve size mm)							M_{DE}*	SZ_{RB}**	LA_{RB}**	DEN_P***	WA_{24}***
		0.063	0.5	22.4	31.5	40	50	63					
Mean	TB	0.13	0.32	0.52	3.40	22.42	62.08	96.63	5.03	15.80	13.58	2.713	0.177
	PS	0.21	0.31	0.44	2.63	20.49	66.98	97.12	9.50	19.25	22.20	2.840	0.480
	W	0.19	0.34	0.76	5.39	28.94	64.33	96.62	0.53	16.27	12.11	2.713	0.123
	RC	0.55	0.96	2.06	5.48	22.68	60.87	95.86	5.75	14.45	11.00	2.690	0.105
H		20.614	12.036	10.202	9.995	12.79	2.582	1.988	5.292	4.907	4.847	0.335	3.251
Asymp. Sig. β		0.001	0.007	0.017	0.019	0.005	0.461	0.575	0.152	0.179	0.183	0.953	0.355

Note: $\chi^2_{0.05} = 81.38$, $\chi^{2*}_{0.05} = 49.80$, $\chi^{2**}_{0.05} = 44.99$.

Table 7
Compliance of experimental data distribution to normal distribution.

Parameter		Methods of testing normal distribution									
		Skew	Conclusion	Kurt	Conclusion	KS	Conclusion	SW	Conclusion	χ^2	Conclusion
Gradation (percent passing)	0.063	2.74	–	10.146	–	0.244	–	0.701	–	83.83	–
	0.5	2.843	–	10.568	–	0.256	–	0.689	–	66.29	+
	22.4	5.461	–	34.674	–	0.313	–	0.417	–	40.81	+
	31.5	3.322	–	16.278	–	0.206	–	0.707	–	13.67	+
	40	0.956	–	0.903	+	0.123	+	0.939	–	4.21	+
	50	0.679	+	0.007	+	0.187	–	0.928	–	5.97	+
	63	−0.255	+	0.289	+	0.09	+	0.959	+	40.11	+
M_{DE}*		1.878	–	4.009	–	0.245	–	0.808	–	10.87	+
SZ_{RB}*		0.521	+	1.395	+	0.092	+	0.958	+	8.78	+
LA_{RB}*		0.489	+	1.598	+	0.128	+	0.933	–	7.33	+
DEN_P**		3.232	–	17.160	–	0.312	–	0.571	–	46.09	–
WA_{24}**		4.870	–	26.211	–	0.305	–	0.447	–	11.09	+

Note: Normal distribution testing by different methods' critical values: triple standard deviation of skewness – $3s_{sk} = 0.906$, $3s^*_{sk} = 1.178$, $3s^{**}_{sk} = 1.243$, five times standard deviation of kurtosis – $5s_{ku} = 2.975$, $5s^*_{ku} = 3.84$, $5s^{**}_{ku} = 4.047$; Kolmogorov-Smirnov – $d_{0.05} = 0.171$, $d^*_{0.05} = 0.226$, $d^{**}_{0.05} = 0.234$; Shapiro-Wilk – w_c=0.947, w^*_c=0.935, w^{**}_c=0.930; Pearson – $\chi^2_{0.05} = 81.38$, $\chi^{2*}_{0.05} = 49.80$, $\chi^{2**}_{0.05} = 44.99$.

3.3. Changes of ballast gradation statistical indicators depending on the sampling location

Regression equations of RB gradation were obtained by applying theoretical mathematical model (Eq. (3)) from experimental data when samples were taken from TB, PS, W and RC (Fig. 9). The largest standard deviation s_{pmax} values were obtained of percent passing through sieves, the means $\bar{p}$ of which make up 50–70%.

The highest homogeneity of the material was obtained in samples taken from TB (s_p = 9.00%, when $\bar{p} \approx 55\%$). On the other hand, the lowest homogeneity of the material was obtained in samples taken from the last stage of the technological process – RC (s_p = 16.03%, when $\bar{p} \approx 58\%$).

Fig. 10 presents the ordinates showing the values of maximum standard deviation obtained from regression equations of different sampling locations, which are reliable as R^2 is close to 1.

The obtained results indicate that when the material is produced in the first sampling, taken from TB, determination coeficient was R^2 = 0.992. When this material was reloaded and transported several times, not only determination coefficient became smaller, but standard deviation became bigger (≈78%).

It means that the quality of this material throughout the technological process became worse and worse (Fig. 10).

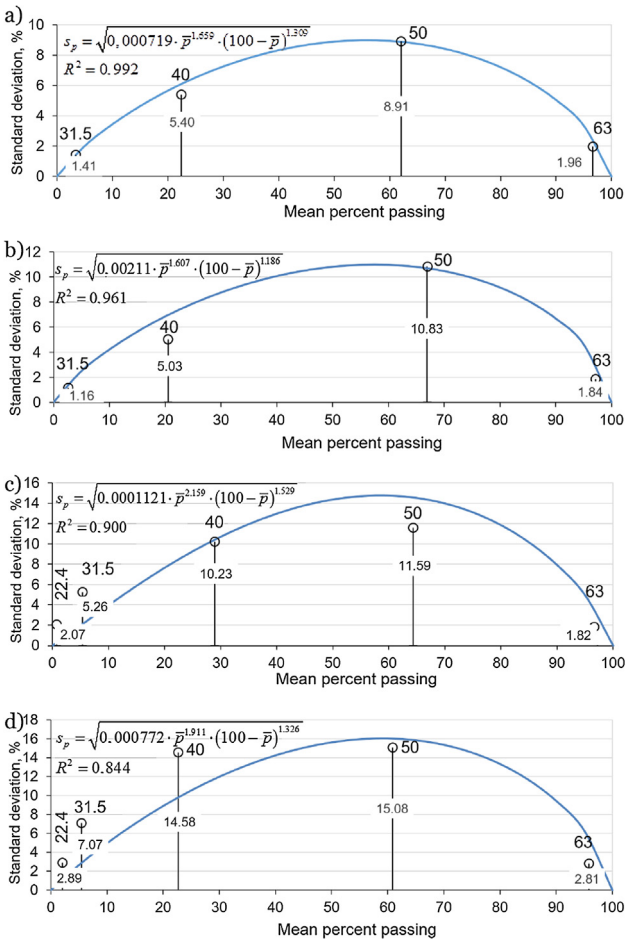

Fig. 9. Correlation between the parameters of ballast material gradation variation (s_p) and position ($\bar{p}$): a – TB; b – PS; c – W; d – RC.

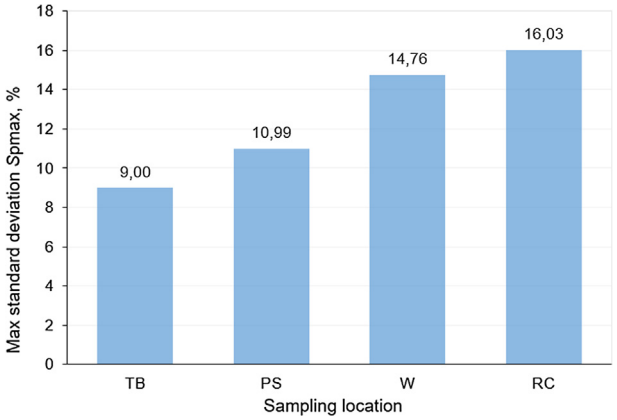

Fig. 10. Differences between the sampling locations according to the max values of standard deviation of percent passing.

3.4. The study of the homogeneity of sampling dispersion

Having grouped samples by four sampling locations TB, PS, W and RC, standard deviations of their gradation showing their differences were obtained (Fig. 11).

The obtained differences indicate that standard deviations of crushed RB gradation percent passing increase when the material is loaded, transported and spread in a layer.

The homogeneity of RB crushed granite was investigated when the material was loaded, transported and laid by comparing the dispersion of four samples' gradation (percent passing). Since four independent samplings complying with normal distribution but varying in size were compared, Bartlett's criterion was employed. Having compared the estimated statistics B (Eq. (5)) with Pearson χ^2(chi-square) statistics with the selected confidence level α and the number of freedom degrees v, null hypothesis was confirmed.

$$B = \frac{E}{C} = \frac{2.303\left[k \cdot \log_{10}\bar{s}^2 - \sum_{i=1}^{l} k_i \log_{10} s_i^2\right]}{1 + \frac{1}{3(l-1)}\left[\sum_{i=1}^{l}\frac{1}{k_i} - \frac{1}{k}\right]} \quad (5)$$

where l – the number of investigated RB crushed stone samples, i.e. the number of sample-taking locations (in this study l = 4); $k_i = n_i$ – 1 – the number of freedom degrees; n_i – the number of investigated samples of i sample-taking location (in this study n_1 = 6, n_2 = 9, n_3 = 32, n_4 = 16); $k = \sum_{i=1}^{l} k_i$; skewed dispersion of s_i^2 sampling percent passing through laboratory sieves; s_i – its standard deviation; $\bar{s}^2$ – weighted mean of sampling dispersions taken from all sample-taking locations (Eq. (6)).

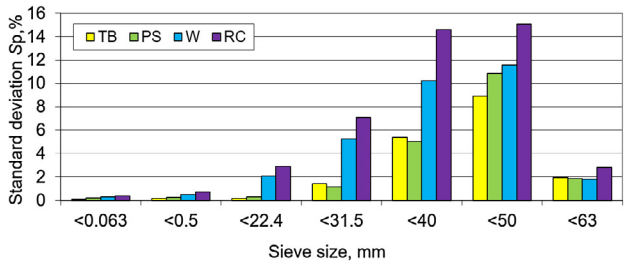

Fig. 11. Differences of standard deviations of RB samples taken in different locations of the technological process.

The mean of weighted dispersions of the samples taken from four technological process locations is calculated as follows:

$$\bar{s}^2 = \frac{\sum_{i=1}^{l} k_i s_i^2}{k}; \quad (6)$$

The value of E = 5.024 and B calculated from the maximum percent passing s_{pmax} presented in Fig. 10 is lower than the critical $\chi^2_{\alpha,\nu}(0.05, 4-1) = 7.82$.Having compared dispersion of percent passing through laboratory sieves from four technological process locations, it was obtained that with the selected significance level they do not differ, and α = 0.05 does not vary statistically (5.024 < 7.82), i. e. they are equal. Therefore, dispersion $\bar{s}^2 = 151.028$and standard deviation $\bar{s} = 12.29\%$calculated by $\bar{s}^2 = 151.028$from all four different sample-taking locations yield average homogeneity of crushed RB in all four sample-taking locations. Notwithstanding, empirical standard deviations s_{pmax} (Fig. 10) and s_p (Fig. 11) tend to increase.

4. Minimum compulsory representative sample size

To identify the gradation or another physical or mechanical quality indicator of heterogeneous crushed RB material, random subsamples, the minimum representative number (number of data) of which is calculated by the following formula [43] are taken:

$$n = \frac{z^2_{\alpha/2} \cdot \sigma^2}{E^2}, \quad (7)$$

where n – the number of samples, $z_{\alpha/2}$– the desired degree of assurance, or probability of success in obtaining the correct answer, measured in standard deviation units from the centre of the t distribution curve; σ– the overall standard deviation of the measurements; E – the maximum allowable difference between the computed average of the measurements and the true average (error).

Suppose Student's distribution duplex test significance level is 95% (the assumed freedom degree number is ∞), then α = 0.05, o $z_{\alpha/2} = 1.96$.

The maximum allowable difference is calculated by the following formula:

$$E = \frac{\delta \cdot \bar{X}}{100}, \quad (8)$$

where δ – allowable relative error (may be 5%, 10%, 15% or 20%); $\bar{X}$– mean of crushed RB quality indicator.

The gradation of crushed RB may be expressed by partial residues on sieves, full screening on sieves and percent passing through sieves. Therefore, the mean calculated for a separate sieve in the three ways presented above, varies. Commonly, the gradation of crushed granite used for RB is expressed by percent passing. Therefore, variation of crushed RB gradation is identified according to the highest value of standard deviation s_{pmax}, which corresponds to the mean $\bar{p}$of percent passing, approximate to 50–70% (Fig. 9).

The selected allowable relative error (δ) is 5%, 10%, 15%, 20%. Table 8 presents the results of calculations.

Maximum standard deviations s_{pmax} were obtained by taking samples from W (14.76%) and from RC (railway construction)

Table 8
Compulsory minimal number of samples to identify properties.

Statistical indicator	Relative error δ (%), when sampling location is																			
	All locations				TB				PS				W				RC			
	5	10	15	20	5	10	15	20	5	10	15	20	5	10	15	20	5	10	15	20
Gradation																				
Mean, %	65				55				55				60				60			
Std. Dev., %	12.59				9.00				10.99				14.76				16.03			
CoV., %	19.37				16.36				19.98				24.6				26.72			
Sample size n	58	15	7	6	42	11	5	3	62	16	7	4	93	24	11	6	110	28	13	7
M_{DE}																				
Mean,	5.48				5.03				9.5				5.25				5.75			
Std. Dev., %	1.72				0.25				1.3				1.49				1.35			
CoV., %	31.39				4.97				13.68				28.38				23.49			
Sample size n	152	38	17	10	4	1	1	1	29	8	4	2	124	31	14	8	85	22	10	6
SZ_{RB}																				
Mean,	16.3				15.8				19.25				16.27				14.45			
Std. Dev., %	1.68				1.06				1.65				1.38				2.25			
CoV., %	10.31				6.71				8.57				8.48				15.57			
Sample size n	17	5	2	2	7	2	1	1	12	3	2	1	12	3	2	1	38	10	5	3
LA_{RB}																				
Mean,	12.44				13.58				20.2				12.11				11			
Std. Dev., %	2.62				0.93				0				2.22				3.3			
CoV., %	21.06				6.85				0				18.33				30			
Sample size n	69	18	8	5	8	2	1	1	1	1	1	1	52	13	6	4	139	35	16	9
DEN_P																				
Mean,	2.72				2.71				2.84				2.71				2.69			
Std. Dev., %	0.061				0.0048				0.17				0.025				0.08			
CoV., %	2.24				0.18				5.99				0.92				2.97			
Sample size n	1	1	1	1	1	1	1	1	6	2	1	1	1	1	1	1	2	1	1	1
WA_{24}																				
Mean,	0.15				0.18				0.48				0.12				0.105			
Std. Dev., %	0.144				0.033				0.43				0.042				0.035			
CoV., %	96				18.33				89.58				35				33.33			
Sample size n	1417	355	158	89	52	13	6	4	1234	309	138	78	189	48	21	12	171	43	19	11

(16.03%), when the mean of percent passing was 60% (Table 8). When allowable relative error δ = 10%, the obtained minimum sample size from W is n = 24 and from railway n = 28.

Minimum standard deviations s_{pmax} were obtained in samples taken from idle TB (transporter belt) (9.00%) and from PS (plant stockpile) (10.99%), when the mean of percent passing was 55% (Table 8). When allowable relative error δ = 10%, the obtained minimum sample size n = 11 from TB and n = 16 from PS.

To identify M_{DE} indicator, minimum representative sample size when δ = 10% by taking samples from idle TB shall be n = 1, from PS – n = 8, from W – n = 31 and from RC – n = 22.

Maximum standard deviations s, SZ_{RB} were obtained by taking samples from RC (2.25%), W (1.38%) and PS (1.65%) (Table 8). When allowable relative error δ = 10%, the obtained minimum sample size from RC was n = 10 and n = 3 from W and PS.

Minimum standard deviation s, SZ_{RB} was obtained from idle TB (1.06%). When allowable relative error δ = 10%, minimal sample size n = 2 was obtained from idle TB.

LA_{RB} maximum standard deviations s were obtained in samples from W (2.22%) and from RC (3.3%) (Table 8). When allowable relative error δ = 10%, minimal sample size n = 13 was obtained from W and n = 35 from RC.

Minimum standard deviations s, LA_{RB} were obtained by sampling from idle TB (0.93%) and from PS (0%). When allowable relative error $\delta = 10\%$, the obtained minimum sample size from idle TB shall be n = 2 and n = 1 from PS.

To identify DEN_P of crushed RB, when $\delta = 5\%$, the minimum representative sample size shall be n = 2, and when δ = (10–20)%, it shall be n = 1 (Table 8).

Water absorption (WA_{24}) of crushed RB is characterized by the greatest variation of all properties: its variation coefficient varied from 89.6% (when sampling from PS) to 18.33% (when sampling from idle TB). Therefore, the greatest number of separate samples n shall be taken to identify this property (Table 8).

This indicates that the porosity/voidness of the material used to produce crushed granite varies.

5. Conclusions

1. RB is constructed of 0/63 crushed granite. The deposits of granite are hardly reachable on the territory of Lithuania; therefore, it is imported from other countries. This material is used to produce crushed RB in the construction or reconstruction of railways in Lithuania. Due to incomplete mixing of crushed granite particles of various size on belt transporter, segregation in a conic stockpile, reloading and transporting processes, the gradation of the produced crushed RB frequently varies from technical specifications. According to the uniformity coefficient of the gradation curve and the rate of curvature, it can be of different variation, the size of which is determined by representative sample-taking of crushed RB.
2. The gradation of crushed RB produced in Lithuania is stipulated by technical specifications of LST EN 13450:2013. To evaluate the dispersion of gradation, it was proposed to use the maximum standard deviation of homogeneous percent passing obtained from the regression equation, which account for 50–70% of the total mass of the mixture. Such value of maximum standard deviation enables to compare crushed stone material of various coarseness and homogeneity. The original method enables to evaluate the range of any aggregate's gradation variation through the use of one number (maximum standard deviation).
3. To lay RB course in railway construction, normal distribution of the crushed granite percent passing M_{DE}, SZ_{RB}, LA_{RB}, DEN_P and WA_{24} was verified according to the criteria of skewness (Skew) and Kurtosis (Kurt), Kolmogorov-Smirnov (KS), Shapiro-Wilk (SW), Pearson (chi-square). Most of these properties comply with the normal distribution, which enables to take into account the variation of crushed RB quality indicators by applying regular criteria of mathematical statistics (Kruskal-Wallis and Bartlett).
4. During the technological processes of loading, transporting and laying the produced crushed RB tends to fine down. The variation of its gradation increases. Standard deviations of crushed granite RB percent passing during various technological processes are equal to the following: TB (9.00%), PS (10.99%), W (14.76%) and RC (16.03%) (from TB to RC max difference about 78%), even though they were not statistically different.
5. The following means of the produced crushed granite RB percent passing through 50 mm laboratory sieve during the stages of the technological process were obtained: TB (62.08%), PS (66.98%), W (64.33%) and RC (60.87%). They did not differ according to Kruskal-Wallis criterion.
6. The estimated minimal representative sample size indicates that separate subsamples shall be taken from RC, not from TB.

Conflict of interest

None.

Appendix

See, Tables 9–12.

Table 9
Compliance of the data obtained from TB distribution with the specifications of normal distribution.

Parameter		Methods of normal distribution testing									
		Skew	Conclusion	Kurt	Conclusion	KS	Conclusion	SW	Conclusion	χ^2	Conclusion
Gradation (percent passing)	0.063	−0.857	+	−0.3	+	0.293	+	0.822	+	1	+
	0.5	1.84	+	3.912	+	0.378	+	0.751	–	1	+
	22.4	0.711	+	−2.052	+	0.286	+	0.755	–	1	+
	31.5	−0.262	–	0.853	+	0.195	+	0.976	+	0	+
	40	0.933	+	0.635	+	0.184	+	0.931	+	0	+
	50	0.534	+	0.914	+	0.192	+	0.970	+	0	+
	63	−0.977	+	2.137	+	0.246	+	0.932	+	0	+
M_{DE}^{*}		−1.846	+	3.412	+	0.353	+	0.744	–	0.5	+
SZ_{RB}^{*}		1.721	+	–	–	0.372	+	0.783	+	0	+
LA_{RB}^{**}		0.538	+	−2.698	+	0.264	+	0.909	+	0	+
DEN_P^{**}		−1.732	+	–	–	0.385	+	0.750	–	0.333	+
WA_{24}^{**}		1.732	+	–	–	0.385	+	0.750	–	0.333	+

Note: Normal distribution testing by different methods' critical values: triple standard deviation of skewness – $3s_{sk} = 2.536$, $3s_{sk}^{*} = 3.043$, $3s_{sk}^{**} = 3.674$, five times standard deviation of kurtosis – $5s_{ku} = 15.152$, $5s_{ku}^{*} = 13.093$, $5s_{ku}^{**} = -$; Kolmogorov-Smirnov – $d_{0.05} = 0.521$, $d_{0.05}^{*} = 0.624$, $d_{0.05}^{**} = 0.708$; Shapiro-Wilk – w_c=0.788, w_c^{*}=0.748, w_c^{**}=0.767; Pearson – $\chi^2_{0.05} = 11.07$, $\chi^{2*}_{0.05} = 7.82$, $\chi^{2**}_{0.05} = 5.99$.

Table 10
Compliance of the data obtained from PC distribution with the specifications of normal distribution.

Parameter		Methods of normal distribution testing									
		Skew	Conclusion	Kurt	Conclusion	KS	Conclusion	SW	Conclusion	χ^2	Conclusion
Gradation (percent passing)	0.063	1.329	+	0.746	+	0.308	+	0.776	–	3.0	+
	0.5	1.616	+	2.704	+	0.220	+	0.817	–	2.333	+
	22.4	1.024	+	−0.089	+	0.223	+	0.872	+	1.111	+
	31.5	1.798	+	3.994	+	0.219	+	0.831	+	0.778	+
	40	1.823	+	4.742	+	0.293	+	0.787	–	–	+
	50	0.656	+	−1.294	+	0.222	+	0.855	–	–	+
	63	−0.174	+	−0.622	+	0.139	+	0.954	–	–	+
$M_{DE}{}^{*}$		–	–	–	0	0.26	+	–	–	–	–
$SZ_{RB}{}^{*}$		–	–	–	0	0.26	+	–	–	–	–
$LA_{RB}{}^{*}$		–	–	–	0	–	–	–	–	–	–
$DEN_{P}{}^{*}$		–	–	–	0	0.26	+	–	–	0.000	–
$WA_{24}{}^{*}$		–	–	–	0	0.26	+	–	–	0.000	–

Note: Normal distribution testing by different methods' critical values: triple standard deviation of skewness – $3s_{sk} = 2.151$, $3s^{*}_{sk} = -$, five times standard deviation of kurtosis – $5s_{ku} = 6.999$, $5s^{*}_{ku} = 0$; Kolmogorov-Smirnov – $d_{0.05} = 0.432$, $d^{*}_{0.05} = 0.975$; Shapiro-Wilk – w_c=0.829, w^{*}_{c}= –; Pearson – $\chi^2_{0.05} = 15.51$, $\chi^{2*}_{0.05} = -$.

Table 11
Compliance of the data obtained from W distribution with the specifications of normal distribution.

Parameter		Methods of normal distribution testing									
		Skew	Conclusion	Kurt	Conclusion	KS	Conclusion	SW	Conclusion	χ^2	Conclusion
Gradation (percent passing)	0.063	1.724	–	3.872	+	0.288	–	0.688	–	23.938	+
	0.5	1.627	–	4.835	–	0.182	+	0.831	–	6.5	+
	22.4	2.444	–	8.44	–	0.214	+	0.728	–	11.875	+
	31.5	0.916	+	0.823	+	0.123	+	0.968	+	5.5	+
	40	0.972	+	0.368	+	0.138	+	0.933	+	0.938	+
	50	0.736	+	−0.261	+	0.195	+	0.937	+	0.937	+
	63	0.406	+	−0.018	+	0.146	+	–	–	11.937	+
$M_{DE}{}^{*}$		2.179	–	7.027	–	0.188	+	0.823	–	7.552	+
$SZ_{RB}{}^{*}$		0.806	+	0.856	+	0.138	+	0.945	+	5.138	+
$LA_{RB}{}^{*}$		0.15	–	1.026	+	0.121	+	0.948	+	5.138	+
$DEN_{P}{}^{**}$		−2.904	–	11.329	–	0.342	–	0.66	–	33.692	+
$WA_{24}{}^{**}$		0.426	+	−0.461	+	0.131	+	0.957	+	10.615	+

Note: Normal distribution testing by different methods' critical values: triple standard deviation of skewness – $3s_{sk} = 1.243$, $3s^{*}_{sk} = 1.301$, $3s^{**}_{sk} = 1.367$, five times standard deviation of kurtosis – $5s_{ku} = 4.047$, $5s^{*}_{ku} = 4.226$, $5s^{**}_{ku} = 4.433$; Kolmogorov-Smirnov – $d_{0.05} = 0.234$, $d^{*}_{0.05} = 0.246$, $d^{**}_{0.05} = 0.259$; Shapiro-Wilk – w_c=0.930, w^{*}_{c}=0.926, w^{**}_{c}=0.920; Pearson – $\chi^2_{0.05} = 44.99$, $\chi^{2*}_{0.05} = 41.34$, $\chi^{2**}_{0.05} = 37.65$.

Table 12
Compliance of the data obtained from RC distribution with the specifications of normal distribution.

Parameter		Methods of normal distribution testing									
		Skew	Conclusion	Kurt	Conclusion	KS	Conclusion	SW	Conclusion	χ^2	Conclusion
Gradation (percent passing)	0.063	1.575	+	3.434	+	0.259	+	0.840	–	6.75	+
	0.5	1.350	+	2.353	+	0.185	+	0.856	–	6.00	+
	22.4	2.907	–	9.228	–	0.337	–	0.603	–	2.00	+
	31.5	2.860	–	8.963	–	0.309	+	0.607	–	0.875	+
	40	1.459	+	1.456	+	0.268	+	0.823	–	0.000	+
	50	0.944	+	0.617	+	0.254	+	0.896	+	0.000	+
	63	−0.158	+	−0.365	+	0.165	+	0.938	+	3.5	+
$M_{DE}{}^{*}$		–	–	–	–	0.26	+	–	–	0.000	+
$SZ_{RB}{}^{*}$		–	–	–	–	0.26	+	–	–	0.000	+
$LA_{RB}{}^{*}$		–	–	–	–	0.26	+	–	–	0.000	+
$DEN_{P}{}^{*}$		–	–	–	–	0.26	+	–	–	0.000	+
$WA_{24}{}^{*}$		–	–	–	–	0.26	+	–	–	0.000	+

Note: Normal distribution testing by different methods' critical values: triple standard deviation of skewness – $3s_{sk} = 1.693$, $3s^{*}_{sk} = -$, five times standard deviation of kurtosis – $5s_{ku} = 5.677$, $5s^{*}_{ku} = -$; Kolmogorov-Smirnov – $d_{0.05} = 0.327$, $d^{*}_{0.05} = 0.842$; Shapiro-Wilk – w_c=0.887, w^{*}_{c}= –; Pearson – $\chi^2_{0.05} = 25.00$, $\chi^{2*}_{0.05} = 3.84$.

References

[1] AB "Lietuvos Geležinkeliai" Annual Report. 2013. Vilnius, Lithuania. Available at: http://www.litrail.lt/documents/10291/19071/LT_19.05_www.pdf/052d58f4-c704-4df5-b288-4e1a6d081295.

[2] H. Sivilevicius, L. Maskeliunaite, Multiple criteria evaluation and the inverse hierarchy model for justifying the Choise of rail transport mode, Promet TrafficTransp. 30 (2018) 157–169, https://doi.org/10.7307/ptt.v30i1.2417.

[3] H. Sivilevicius, L. Maskeliunaite, The numerical example for evaluating the criteria describing the quality for the trip by international train, E&M Econ. Manage. 17 (2) (2014) 73–86, https://doi.org/10.15240/tul/001/2014-2-006.

[4] L. Maskeliūnaitė, H. Sivilevičius, The model for evaluating the criteria describing the quality of the trip by international train, Technol. Econ. Dev. Econ. 20 (3) (2014) 484–506, https://doi.org/10.3846/20294913.2014.949333.

[5] R. Janardhanam, C.S. Desai, Three-dimensional testing and modeling of ballast, J. Geotech. Eng. 109 (6) (1983) 783–796, https://doi.org/10.1061/(ASCE)0733-9410(1983) 109:6(783).

[6] L. Bai, R. Liu, Q. Sun, F. Wang, P. Xu, Markov – based model for the prediction of railway track irregularities, Proc. Inst. Mech. Eng. Part F: J. Rail Rapid Transit 229 (2) (2015) 150–159, https://doi.org/10.1177/0954409713503460.
[7] I. Arasteh Khouy, P. Larsson-Kraik, A. Nissen, U. Juntti, H. Schunnesson, Optimisation of track geometry inspection interval, Proc. Inst. Mech. Eng. Part F: J. Rail Rapid Transit. 228 (5) (2014) 546–556, https://doi.org/10.1177/0954409713484711.
[8] P. Xu, Q. Sun, R. Liu, F. Wang, A short-range prediction model for track quality index, Proc. Inst. Mech. Eng. Part F: J. Rail Rapid Transit. 225 (3) (2011) 277–285, https://doi.org/10.1177/2041301710392477.
[9] B. Counter, A. Abu-Tair, A. Franklin, D. Tann, Refurbishment of ballasted track systems; the technical challenges of quality and decision support tools, Constr. Build. Mater. 92 (2015) 51–57, https://doi.org/10.1016/j.conbuildmat.2014.11.036.
[10] M. Esmaeili, S. Amiri, K. Jadidi, An investigation into the use of asphalt layers to control stress and strain levels in railway track foundations, Proc. Inst. Mech. Eng. Part F: J. Rail Rapid Transit. 225 (2) (2014) 182–193, https://doi.org/10.117/0954409712468850.
[11] B. Indraratna, D. Ionescu, H.D. Christie, Shear behavior of railway ballast based on large-scale triaxial tests, J. Geotech. Geoenviron. Eng. 124 (5) (1998) 439–449.
[12] D. Navikas, M. Bulevičius, H. Sivilevičius, Determination and evaluation of railway aggregate sub-ballast gradation and other properties variation, J. Civ. Eng. Manage. 22 (5) (2016) 699–710, https://doi.org/10.3846/13923730.2016.1177586.
[13] A. López-Pita, P.F. Teixeira, C. Casas, A. Bachiller, P.A. Ferreira, Maintenance costs of high-speed lines in Europe, Transp. Res. Rec. 2043 (2008) 13–19, https://doi.org/10.1016/j.retrec.2012.03.011.
[14] A. Berghold, P. Veit, Track service life – driven by ballast quality in 1st Railway Track Science and Engineering International Workshop – Ballast: Issues and Challenges. UIC Paris 2013 (2013).
[15] G.P. Raymond, R.J. Bathurst, Performance of large-scale model single tie-ballast systems, Transp. Res. Rec. 1131 (1987) 7–14.
[16] Y. Haddani, G. Saussine, R. Gourvès, Field ballast granuliometry assessment thanks to image analysis in 1st Railway Track Science and Engineering International Workshop – Ballast: Issues and Challenges. UIC Paris 2013, 2013. Available at: http://www.rtse-workshops.org/.
[17] I. Gallego, J. Munoz, S. Sanchez-Cambronero, A. Rivas, Recommendations for numerical rail substructure modeling considering nonlinear elastic behavior, J. Transp. Eng. 13 (2013) 848–858.
[18] T. V. Duong, A. M. Tang, Y. J. Cui, J. C. Dupla, J. Canou, N. Calon, A. Robinet, The interaction between ballast and underlying layer in railway sub-structure in 1st Railway Track Science and Engineering International Workshop – Ballast: Issues and Challenges. UIC Paris 2013, 2013.
[19] E.T. Selig, J.M. Waters, Track Geotechnology and Substructure Management, Thomas Telford Services Ltd., London, 1994.
[20] A. Aikawa, Dynamic characterization of a ballast layer subject to traffic impact loads using free-dimensional sensing stones and special sensing sleeper, Constr. Build. Mater. 92 (2015) 23–30, https://doi.org/10.1016/j.conbuildmat.2014.06.005.
[21] J. Kennedy, P.K. Woodward, G. Medero, M. Banimahd, Reducing railway track settlement using three-dimensional polyurethane polymer reinforcement of the ballast, Constr. Build. Mater. 44 (2013) 615–625, https://doi.org/10.1016/j.conbuildmat.2013.03.002.
[22] M. Sol-Sánchez, N.H. Thom, F. Moreno-Navarro, M.C. Rubio-Gámez, G.D. Airey, A study into the use of crumb rubber in railway ballast, Constr. Build. Mater. 75 (2015) 19–24, https://doi.org/10.1016/j.conbuildmat.2014.10.045.
[23] I. Arasteh Khouy, H. Schunnesson, U. Juntti, A. Nissen, P. Larsson-Kraik, Evaluation of track geometry maintenance for a heavy haul railroad in Sweden: a case study, Proc. Inst. Mech. Eng. Part F: J. Rail Rapid Transit. 228 (5) (2014) 496–503, https://doi.org/10.1177/0954409713482239.
[24] C. Vale, I.M. Ribeiro, R. Calçada, Integer programming to optimize tamping in railway tracks as preventive maintenance, J. Transp. Eng. 138 (1) (2012) 123–131, https://doi.org/10.1061/(ASCE)TE.1943-5436.0000296.
[25] L.F. Caetano, P.F. Teixeira, Predictive maintenance model for ballast tamping, J. Transp. Eng. 142 (4) (2016) 04016006, https://doi.org/10.1061/(ASCE)TE.1943-5436.0000825.
[26] A.R. Andrade, P.F. Teixeira, A Bayseian model to assess rail track geometry degradation through its life-cycle, Res. Transp. Econ. 36 (2012) 1–8, https://doi.org/10.1016/j.retrec.2012.03.011.
[27] M. Bulevičius, K. Petkevičius, S. Čirba, The influence of geometric parameters on strength properties of the aggregates used to produce asphalt mixtures, J. Civ. Eng. Manage. 19 (6) (2013) 894–902, https://doi.org/10.3846/13923730.2013.858645.
[28] H. Huang, E. Tutumluer, Image – aided element shape generation method in discrete – element modeling for railroad ballast, J. Mater. Civ. Eng. 26 (3) (2014) 527–535, https://doi.org/10.1061/(ASCE)MT.1943-5533.0000839.
[29] M. Moaveni, S. Wang, J.M. Hart, E. Tutumluer, N. Ahuja, Evaluation of aggregate size and shape by means of segmentation techniques and aggregate image processing algorithms, Transp. Res. Rec. 2335 (2013) 50–59, https://doi.org/10.3141/2335-06.
[30] I.S. Bessa, V.T.F. Castelo Branco, J.B. Soares, Evaluation of polishing and degradation resistance of natural aggregates and steel slag using the aggregate image measurement system, Road Mater. Pavement Des. 15 (2) (2014) 385–405, https://doi.org/10.1080/14680629.2014.883323.
[31] T.F. Yideti, B. Birgisson, D. Jelagin, Influence of aggregate packing structure on California bearing ratio values of unbound granular materials, Road Mater. Pavement Des. 15 (1) (2014) 102–113, https://doi.org/10.1080/14680629.2013.863160.
[32] Y. Cui, T.V. Duong, A.M. Tang, J.C. Dupla, N. Calon, A. Robinet, Investigation of the hydro-mechanical behaviour of fouled ballast, J. Zhejiang Univ. 14 (4) (2013) 244–255.
[33] S. Nimbalkar, B. Indraratna, S.K. Dash, D. Christie, Improved performance of railway ballast under impact loads using shock mats, J. Geotech. Geoenviron. Eng. 138 (3) (2012) 281–294, https://doi.org/10.1061/(ASCE)GT.1943-5606.0000598.
[34] Y.F. Sun, Y. Xiao, W. Ju, Bounding surface model for ballast with additional attention on the evolution of particle size distribution, Sci. China Technol. Sci. (2014), https://doi.org/10.1007/s11431-014-5575-4.
[35] B. Indraratna, W. Salim, C. Rujikiatkamjorn, Advanced Rail Geotechnology – Ballasted Track, A.A. Balkema-Taylor and Francis, UK, 2011.
[36] B. Indraratna, S. Nimbalkar, M. Coop, S.W. Sloan, A constitutive model for coal-fouled ballast capturing the effects of particle degradation, Comput. Geotech. 61 (2014) 96–107, https://doi.org/10.1016/j.compgeo.2014.05.003.
[37] M. Stahl, H. Konietzky, Discrete element simulation of ballast and gravel under special consideration of grain-shape, grain-size and relative density, Granular Matter 13 (2011) 417–428.
[38] Y. Xiao, H.L. Liu, G. Yang, Y.M. Chen, J.S. Jiang, A constitutive model for the state-dependent behaviors of rockfill material considering particle breakage, Sci. China Technol. Sci. 57 (2014) 1636–1646, https://doi.org/10.1007/s11431-014-5601-6.
[39] LST EN 13450: 2013. Aggregates for railway ballast. 33p.
[40] K.A. Skoglund, Dissertation, A Study of Some Factors in Mechanistic Railway Track Design, 2002.
[41] LST EN 1331: 2015. Soils for use in road construction – Classification
[42] D. Mučinis, H. Sivilevičius, R. Oginskas, Factors determining the inhomogeneity of reclaimed asphalt pavement and estimation of its components content variation parameters, Baltic J. Road Bridge Eng. 4 (2) (2009) 69–79, https://doi.org/10.3846/1822-427X.2009.4.69-79.
[43] D.C. Montgomery, G.C. Runger, Applied Statistics and Probability for Engineers, second ed., John Wiley & Sons, Inc., New York, 1999, p. 817p.
[44] W.J. Conover, Practical Nonparametric Statistics, third ed., John Wiley & Sons, Inc New York, 1999, pp. 428–433.
[45] R.G. Jr, Miller, Beyond ANOVA, Basics of Applied Statistics, John Wiley & Sons, New York, 1986.
[46] A. Madansky, Prescription for Working Statisticians, Springer-Verlag, New York, 1988.
[47] N.M. Razali, Y.B. Wah, Power comparsions of Shapiros-Wilk Kolmogorov-Smirnov, Lilliefors and Anderson-Darling tests, J. Stat. Model. Anal. 2 (1) (2011) 21–33.
[48] S.S. Shapiro, M.B. Wilk, An analysis of variance test for normality (Complete Samples), Biometrica. 52 (3/4) (1965) 591–611.